Probing the Local Structure and the Role of Protons in Lithium Sorption Processes of a New Lithium-Rich Manganese Oxide

María J. Ariza,*[,†,‡] Deborah J. Jones,[†] Jacques Rozière,[†] Ramesh Chitrakar,[§] and Kenta Ooi[§]

Laboratoire des Agrégats Moléculaires et Matériaux Inorganiques, UMR CNRS 5072, Université Montpellier II, Place Eugène Bataillon, 34095 Montpellier Cédex 5, France, and Shikoku National Industrial Research Institute, 2217-14 Hayashi-cho, Takamatsu 761-0395, Japan

Received October 5, 2005. Revised Manuscript Received December 19, 2005

Lithium exchange mechanisms, local structure, and its possible evolutions on lithium extraction and reinsertion are studied in $Li_{1.6}Mn_{1.6}O_4$, a new lithium-rich manganese oxide showing improved lithium sorption. The parent $Li_{1.6}Mn_{1.6}O_4$ and its lithium-extracted and lithium-reinserted forms are characterized by X-ray absorption (EXAFS and XANES) and incoherent inelastic neutron scattering (IINS) spectroscopies. Lattice hydroxyl groups are detected in the lithium-extracted sample; the chemical reinsertion of lithium removes most of the hydroxyl groups, but some protons remain in the structure mainly as structural water. X-ray absorption spectroscopy at the manganese K-edge indicates a local spinel structure of $Li_{1.6}Mn_{1.6}O_4$ with manganese in oxidation state 4+. The structural arrangement and Mn oxidation state remain unchanged when lithium is extracted and reinserted. The lithium sorption occurs by Li^+/H^+ ion exchange process, as for $Li_{1.33}Mn_{1.67}O_4$, the previously considered end member of the $Li_{1+x}Mn_{2-x}O_4$ spinel lithium-rich series. Since the cation-to-anion ratio of $Li_{1.6}Mn_{1.6}O_4$ is not that which is typical for a spinel, the new lithium-rich manganese oxide has a spinel structure with the extra Li^+ probably in interstitial sites, although lithium cannot be located unequivocally from these results.

Introduction

Manganese oxides derived from lithium-rich manganese oxide spinels are promising inorganic adsorbents for extracting lithium from seawater,[1] which is considered one of the vaster sources of this metal widely used nowadays for batteries. A wide range of stoichiometric lithium-rich manganese oxide spinels having the general formula $Li_{1+x}Mn_{2-x}O_4$, where $0 \leq x \leq 0.33$ can be prepared by solid-phase reaction. $LiMn_2O_4$ ($x = 0$) is the ideal cubic spinel, where the average oxidation state of Mn is 3.5+. Manganese and oxygen sites are 16d and 32e (space group $Fd\bar{3}m$), respectively, and lithium ions can be removed and reinserted at 8a sites within the octahedral sublattice while retaining the spinel framework. On increasing the value of x, so-called lithium-rich spinels are obtained, where Li ions substitute Mn in octahedral 16d sites[2,3] and the mean oxidation state of Mn increases until the average manganese oxidation state is close to 4+ (Mn^{IV}), which occurs for $x = 0.33$. However, a new lithium-rich manganese oxide having the formula $Li_{1.6}Mn_{1.6}O_4$ has been synthesized from the oxidation of a phase prepared by a hydrothermal route.[4] Its lithium-extracted form exhibits higher lithium uptake from Li-enriched seawater than $LiMn_2O_4$ and $Li_{1.33}Mn_{1.67}O_4$ lithium-extracted materials.[5] X-ray diffraction revealed a spinel-type structure for $Li_{1.6}Mn_{1.6}O_4$ with a lattice constant of 8.14 Å, but the relative intensity of diffraction peaks differs slightly from that of previous spinel manganates.[5] Moreover, the cation/anion ratio in this phase ($r_{c/a} = 1$) is higher than that of a typical spinel ($r_{c/a} = 0.75$), which suggests the structure to be either hexagonal or spinel with oxygen vacancies or interstitial cations. Then the structure of the new lithium manganate is not unequivocally identified by X-ray diffraction (XRD), and further studies are required to elucidate between a cubic spinel structure with interstitial Li or oxygen deficiency and a hexagonal one with cation deficiency.

The mechanism of lithium extraction/insertion of $Li_{1+x}Mn_{2-x}O_4$ compounds in aqueous solutions has been extensively studied. For $LiMn_2O_4$ ($Mn^{III}/Mn^{IV} = 1$) lithium extraction is mainly a redox reaction, while for $Li_{1.33}Mn_{1.67}O_4$ (all Mn^{IV}) it involves essentially a lithium by proton ion exchange process,[3,6−7] giving a protonated manganese oxide ($MnO_2 \cdot 0.31H_2O$). In the new lithium-rich manganate, the oxidation state of Mn is 4+, and a Li^+/H^+ ion-exchange mechanism has been proposed for lithium extraction and reinsertion.[5] The effectiveness of water absorption of $Li_{1.6}Mn_{1.6}O_4$ is also higher, giving $MnO_2 \cdot 0.5H_2O$. Infrared spectra

* Corresponding author:. E-mail: mjariza@ual.es. FAX: +34 950 015434.
† Université Montpellier II.
‡ Current address: Grupo de Física de Fluidos Complejos, D. Física Aplicada, Universidad de Almería, E-04120 Almería, Spain.
§ Shikoku National Industrial Research Institute.

(1) Chitrakar, R.; Kanoh, H.; Miyai, Y.; Ooi, K. *Ind. Eng. Chem. Res.* **2001**, *40*, 2054.
(2) Takada, T.; Akiba, E.; Izumi, F.; Chakoumakos, B. C. *J. Solid State Chem.* **1997**, *130*, 74.
(3) Ammundsen, B.; Jones, D. J.; Rozière, J.; Berg, H.; Tellgren, R.; Thomas, J. O. *Chem. Mater.* **1998**, *10*, 0, 1680.
(4) Tabuchi, M.; Ado, K.; Masquelier, C.; Matsubara, I.; Sakaebe, H.; Kageyama, H.; Kobayashi, H.; Kanno, R.; Nakamura, O. *Solid State Ionics* **1996**, *89*, 53.
(5) Chitrakar, R.; Kanoh, H.; Miyai, Y.; Ooi, K. *Chem. Mater.* **2000**, *12*, 3151.
(6) Ammundsen, B.; Aichison, P. B.; Burns, G. R.; Jones, D. J.; Rozière, J. *Solid State Ionics* **1997**, *97*, 269.
(7) Ammundsen, B.; Jones, D. J.; Rozière, J.; Burns, G. R. *Chem. Mater.* **1995**, *7*, 2151.

10.1021/cm052214r CCC: $33.50
Published on Web 02/15/2006

Table 1. Chemical Composition and Manganese Oxidation State Obtained from Chemical Analysis of the Parent, Delithiated, and Relithiated Lithium-Rich Manganate

	Li/Mn	Z_{Mn}[a]	formula
$Li_{1.6}$(p)	0.99	3.96	$Li_{1.59}Mn_{1.61}O_4$
$Li_{1.6}$(d)	0.014	4.02	$MnO_2 \cdot 0.5H_2O \cdot 0.01Li_2O$
$Li_{1.6}$(r)	0.764	3.99	$Li_{1.29}Mn_{1.68}O_4 \cdot 0.36H_2O$

[a] Standard deviation of three measurements ≤ 0.01.

have shown absorption bands that could be assigned to stretching vibrations of hydroxyl groups in the lattice, but this technique is not specific for protons and it is not able to clearly distinguish between different types of protonated species. Moreover, those infrared bands corresponding to deformation vibrations were not observed.[5] In summary, the nature of protonic species and the proton exchange mechanism is not yet clear.

In this work, we study both the role of protons in lithium extraction/insertion mechanisms and the local structure of $Li_{1.6}Mn_{1.6}O_4$ and their lithium-extracted and -reinserted products using specific techniques sensitive to protons and the local crystal structure. Incoherent inelastic neutron scattering (IINS) is used to probe protons. IINS is a powerful technique for studying protonic species, due to the light mass of protons and the high incoherent scattering cross-section for hydrogen (80.26×10^{-28} m^2) compared with most of the other atoms (0.4×10^{-28} m^2 for Mn and 0.92×10^{-28} m^2 for Li, for example).[8] X-ray absorption is used to study the local structure around manganese. X-ray absorption near-edge spectroscopy (XANES) gives reliable information about the oxidation state of the absorbing atoms and in some cases about the local structure, while the fine structure after the edge (EXAFS) provides local structural information.[9] The evolution of the local structure when lithium is extracted and reinserted is studied through characterization of $Li_{1.6}Mn_{1.6}O_4$ and its lithium-extracted and lithium-reinserted materials.

Experimental Section

Samples. The $Li_{1.6}Mn_{1.6}O_4$ parent ($Li_{1.6}$(p)) was prepared by heating the orthorhombic $LiMnO_2$ precursor, which was prepared hydrothermally at 400 °C for 4 h in air.[4] The thermal treatment of $LiMnO_2$ provokes the oxidation of trivalent manganese to tetravalent ($LiMnO_2 + {}^1/_4O_2 \rightarrow LiMnO_{2.5}$). The Li/Mn ratio of the parent sample is 0.99 ($Li_{1.59}Mn_{1.61}O_4$), as determined by atomic absorption spectroscopy. The oxidation number of Mn determined by the standard oxalic method is 3.96 [5]. The lithium was extracted by stirring the parent sample in 0.5 mol dm^{-3} HCl for 1 day. After acid treatment, the powder was water-washed, recovered, and dried at 60 °C. Part of the lithium-extracted sample was lithium-reinserted, following a similar treatment with an aqueous LiCl solution. Table 1 summarizes the chemical composition of the materials. $Li_{1.6}$(d) and $Li_{1.6}$(r) refer to the lithium-extracted or "delithiated" and lithium-reinserted or "relithiated" samples, respectively. The manganese oxidation state determined by titration is very close to 4 in all cases. Even if $Li_{1.6}$(d) is the best inorganic adsorbent of lithium ions to date,[1] the Li/Mn atomic ratio of $Li_{1.6}$(r) indicates that lithium is only partly reinserted.

Incoherent Inelastic Neutron Scattering. IINS experiments were performed at the pulsed neutron source ISIS (Rutherford Appleton Laboratory (RAL), U.K.). The transfer energy ($E = E_1 - E_0$) from the incident neutrons ($10^{-3} \leq E_0$ (eV) ≤ 1) to the sample was measured using the TOSCA spectrometer. The energy resolution from 5 to 500 meV ($\sim$40 to 4000 cm^{-1}) is approximately 1.5−2% of the energy transfer. Time-of-flight data were converted into energy data using standard analysis procedures implemented in routines at ISIS.[10] Results shown here correspond to neutrons backscattered by the sample at 138.5°. About 3 g of sample were precisely weighed before transferring to thin-walled aluminum holders having the neutron beam size (4×4 cm^2) that were fixed to the center stick of a closed-cycle refrigerator. The spectra were recorded below 30 K and under dynamic vacuum ($\sim$2 mbar) up to approximately 2000 μA h of total integrated current. The IINS spectra were normalized by taking into account the mass of the sample in the beam after subtraction of an experimental background.

X-ray Absorption Spectroscopy. X-ray absorption experiments were performed using the EXAFS-13 spectrometer, line D42, of the DCI storage ring at LURE (Paris Sud University), using synchrotron radiation and a double crystal monochromator with Si^{311} crystals. The monochromator energy resolution is 0.3 eV in the energy range of the manganese K-edge ($E_0 = 6539$ eV). The energy was calibrated using a standard Mn foil by assigning E_0 to the first inflection point of the absorption edge. The XANES spectra were recorded from ca. 100 eV before to 100 eV after the edge with a step size of 0.3 eV. For the EXAFS spectra, the energy step was 2.0 eV from ca. 100 eV before to 1000 eV after the edge. The experiments were performed in transmission mode using ionization chambers partially filled with He/Ne for determining the X-ray intensity before and after the sample (I_0 and I_1, respectively), allowing calculation of the absorption spectra $\mu(E)$. Samples were diluted in boron nitride, and the powder was then mixed with paraffin oil to give a paste that was pressed between two Parafilm windows and fixed in a stainless sample holder that was placed in a coldfinger cryostat (77 K) to record X-ray absorption spectra under dynamic vacuum. The edge jump in each case was close to 1.

Experimental data were analyzed using the software *EXAFS pour le Mac* developed by Michalowicz.[11] The analysis protocol includes the following: (i) extraction of the EXAFS signal $\chi(k) = (\mu - \mu_1)/(\mu_1 - \mu_0)$ where the background before the absorption edge (μ_0) was determined by linear fitting and μ_1 was modeled by a spline polynomial beyond the edge; (ii) calculation of the radial distribution-like function $F(R)$ by fast Fourier transformation (FT) using a Kaiser window ($\tau = 3.5$) over the range of 3−14 Å^{-1} and k^3 weighting; (iii) filtering of different coordination spheres in $F(R)$ (filtering interval of 2.10 Å) and back-Fourier transformation to obtain partial components of the EXAFS spectra; (iv) multivariate least-squares fitting of the filtered spectra in k space from 3.5 to 14.0 Å^{-1} and using calculated photoelectron phase and amplitude functions.[12] The number of neighbors (N_i), interatomic distances (R_i), and Debye−Waller-type factors (σ_i), were then refined for each shell of atoms. Other adjustable parameters, related with the electron mean free path and the overall amplitude reduction, were preliminarily refined for the Li1.6(p) sample by taking into account expected values for lithium manganates[13] and then fixed during the refinement of structural parameters of all the samples. Small

(8) Incoherent scattering cross-section can be found at: http://www.ncnr.nist.gov/resources/n-lengths/.

(9) *X-ray Absorption: Principles, Applications, Techniques of EXAFS, SEXAFS and XANES*; Koningsberger, D. C., Prins, R., Eds.; Wiley: New York, 1988.

(10) Colognesi, D.; Parker, S.; Tomkinson, J. *TOSCA Manual*; ISIS, Rutherford Appleton Laboratory: Chilton, U.K., 2000.

(11) Michalowicz, A. *Logiciels pour la Chimie*; Société Française de Chimie: Paris, 1991.

(12) McKale, A. G.; Veal, B. W.; Paulikas, A. P.; Chan, S. K.; Knapp, G. S. *J. Am. Chem. Soc.* **1988**, *110*, 3763.

(13) Ammundsen, B.; Jones, D. J.; Rozière, J.; Burns, G. R. *Chem. Mater.* **1996**, *8*, 2799.

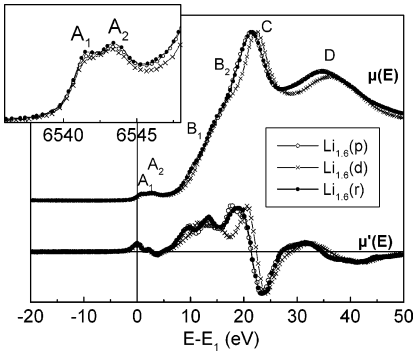

Figure 1. XANES spectra (top) and first derivative curves (bottom) of $Li_{1.6}Mn_{1.6}O_4$ parent, lithium-extracted, and lithium-reinserted samples. The inset shows details of the preedge features not shifted in energy.

adjustments of the energy origin ($2 < \Delta E_0 < 5$ eV) were necessary for each spectrum to obtain a fitting residue ($r = \sum_k [(k\chi_{exp}(k) - k\chi_{th}(k))^2k^3]/\sum_k [(k\chi_{exp}(k))^2k^3]$)[11,14] lower than 1%.

Results and Discussion

Local Structure and Its Evolution with Lithium Extraction and Reinsertion. *XANES.* The X-ray absorption near-edge spectra (top) and their first derivative curves (bottom) of the $Li_{1.6}Mn_{1.6}O_4$, delithiated, and relithiated materials are shown in Figure 1. For comparison, XANES spectra have been shifted to set the first inflection point at zero energy and normalized at the maximum value. The inset of Figure 1 (not energy shifted) shows that the first inflection point in the preedge features is almost coincident for all the three samples at 6541 eV. Since the X-ray absorption edge is very sensitive to the oxidation state of the absorbing atom, this indicates that the oxidation state of manganese atoms remains unchanged under lithium extraction and reinsertion,. The comparison with the edge positions of reference manganese oxides β-MnO_2 (Mn^{IV}) and $LiMn_2O_4$ ($Mn^{III/IV}$) [13] allows us to conclude that manganese atoms are mainly Mn^{IV} in the parent, delithiated, and relithiated $Li_{1.6}Mn_{1.6}O_4$.

Three types of features can be distinguished in the XANES region. Preedge peaks A_1 and A_2 appear in the K-edges of most of the 3d elements due to transitions to bound final states in 3d orbitals. B_1 and B_2 in the rising edge have been associated with medium- or long-range order in compounds with spinel structure.[15] The first and second maxima after the edge (C and D) could be affected by the contraction or expansion of the unit cell. Table 2 lists the energy values of all these features for the three samples. The position of B_1 and B_2 was determined from maxima in the derivative curves.

The spectra of the parent and relithiated samples are very similar, while both features on the edge (B_1 and B_2) and the resonances (C, D) are shifted toward higher energies in the lithium-extracted material. The shift of resonances C and D signals a reversible change of the unit cell dimension. The shift of features in the rising edge is similar to that observed in the extraction of lithium by acid washing of $Li_{1.33}Mn_{1.67}O_4$,[13] and it should be related to the long-range crystal structure and, in particular, to the fractional coordinate of oxygen atoms.

EXAFS. The extended X-ray absorption fine structure spectra of $Li_{1.6}Mn_{1.6}O_4$ parent, delithiated, and relithiated samples are plotted in Figure 2. The parent and relithiated materials have very similar EXAFS oscillations, and only small differences both in phase and amplitude are observed in the delithiated sample. Figure 3 shows the imaginary part (oscillating line) and modulus (envelope) of the Fourier transform of EXAFS signals (not corrected for phase shift). The main maxima at ca. 1.6 and 2.6 Å are identified respectively as the first shell of oxygen atoms and the second shell of manganese atoms in spinel manganese oxides.[13] Maxima at further distances can be associated with the second nearest neighbor oxygen (open circles in the figure) and manganese (asterisk) shells, and they might be affected by multiple scattering. However, multiple scattering can be neglected for the determination of structural parameters of nearest oxygen and manganese neighbors.[13] The peak below 0.5 Å has no physical meaning, and it can be ignored.

To refine the structural parameters of the two first shell of atoms, i.e., interatomic distances and coordination numbers, the main peaks of the FT (between vertical lines in Figure 3) were filtered and inverse Fourier transformed to obtain Fourier filtered EXAFS spectra (scatter points in Figure 4). Coordination numbers (N_i) determined by EXAFS are the structural parameter with less precision (errors may be as large as 20%), and they tend to correlate with the pseudo-Debye−Waller factors (σ_i) in the refinements. The initial values of N_i were selected by taking into account the stoichiometry of $Li_{1.6}Mn_{1.6}O_4$ and assuming either an excess of Li in 16c interstitial sites (case 1: $N_1 = 6.0$ and $N_2 = 4.8$) or an oxygen deficiency (case 2: $N_1 = 5.6$ and $N_2 = 4.5$). In both cases, N_1 converges at 5.8 and N_2 at 4.8 after the fitting procedure. These values are within expected N_i errors but are slightly closer to the former model. Interatomic distances obtained in both cases are almost coincident since small changes in the coordination number are well-accommodated by small changes in the Debye−Waller-type factor, the parameter reflecting the disorder around the central atom.

To compare the parent, lithium-extracted, and lithium-reinserted samples, the three spectra were fitted starting from case 1 conditions. Table 3 lists the interatomic distances (R_i) and the pseudo Debye−Waller factors (σ_i) of the first oxygen (Mn−O) and manganese (Mn−Mn) shells of atoms. Figure 4 shows experimental (symbols) and simulated (solid lines) filtered EXAFS data (top) and the FT moduli (bottom) of the three samples. The agreement between experimental and fitted data is very good not only in the EXAFS spectra (χ-(k)) but also in the position and intensity of the peaks of the pseudo-radial-distribution function. As expected from almost coincident EXAFS spectra, the refined structural parameters are within expected errors for all three samples. Debye−Waller factors of the first shell between 0.065 and 0.068 Å are similar to those reported previously for the couple of Mn^{IV}−O.[13] The distribution of Mn−Mn distances seems to increase slightly with the lithium extraction and reinsertion process, as shown by σ_2 values, while the average distance (R_2) contracts and expands very slightly when lithium is

(14) A summary of error analysis procedures used by Michalowicz software can be found at the International XAFS Society web page: http://scon155.phys.msu.su/~IXS/survey/errors/EA_Survey_Text.html.

(15) Ammundsen, B.; Jones, D. J.; Rozière, J. *J. Solid State Chem.* **1998**, *141*, 294.

Table 2. Energy Position Referred to the First Inflection Point on the Edge of the Main Features in the XANES Spectra (eV)

	A_1	A_2	B_1	B_2	C	D
$Li_{1.6}$(p)	0.9	2.7	9.9	13.5	21.4	34.6
$Li_{1.6}$(d)	0.8	2.8	11.7	14.4	22.4	36.0
$Li_{1.6}$(r)	0.8	2.7	9.8	13.5	21.4	34.6

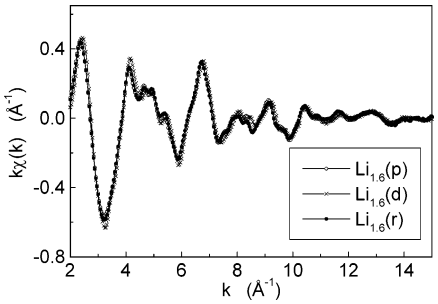

Figure 2. EXAFS spectra of $Li_{1.6}Mn_{1.6}O_4$, delithiated and relithiated samples.

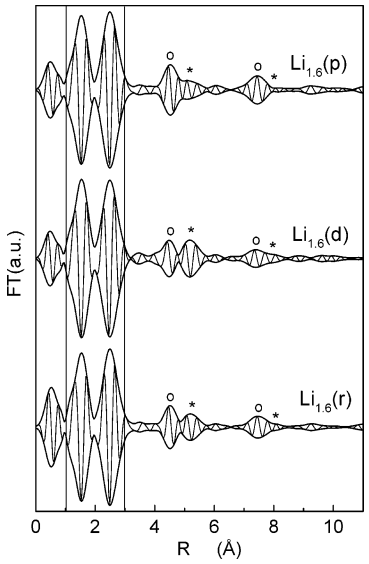

Figure 3. Fourier transformed EXAFS spectra of $Li_{1.6}Mn_{1.6}O_4$, lithium-extracted and lithium-reinserted samples. The oscillating trace is the FT imaginary part; maxima marked by ○ and * correspond to the second and third oxygen and manganese coordination spheres, respectively.

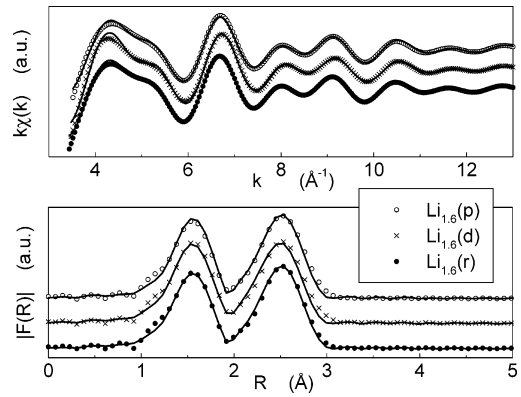

Figure 4. Experimental (symbols) and simulated (solid lines) filtered EXAFS spectra (top) and modulus of the radial distribution function (bottom) of parent, delithiated, and relithiated samples.

extracted and reinserted. These results are consistent with the contraction and expansion of the unit cell detected by powder X-ray diffraction at long-range scale.[5]

Lithium Extraction and Reinsertion Mechanism: Role of Protons. The incoherent and inelastic neutron scattering technique is especially sensitive to protons. Figure 5 shows the IINS spectra of the $Li_{1.6}Mn_{1.6}O_4$ parent, lithium-extracted, and lithium-reinserted samples. The parent sample has a weak IINS spectrum with the main maximum at 450 cm^{-1} corresponding to vibrations of MnO_6 octahedron activated by hydrogen atoms of water (Mn−O−H).[7,16−18] In the lithium-extracted sample ($Li_{1.6}$(d)), the spectrum changes notably since the overall background increases and an intense peak at 909 cm^{-1} and possibly a weaker one at 1087 cm^{-1} appear. Both peaks can be attributed to hydroxyl group deformation (γ(OH)).[5,7,16−17] These assignments are good confirmation that the lithium extraction is a lithium-by-proton-exchange mechanism. Two other groups of signals (at 600 and 675 cm^{-1}) can be assigned to water libration modes, which usually appear between 400 and 800 cm^{-1}. Two maxima of low intensity at around 1560 and 1800 cm^{-1} are also observed. However, IINS spectra are very difficult to assign with accuracy above 1200 cm^{-1}, since the contribution from fundamental vibrations is very low and any appreciable intensity generally arises from overtones and combinations. After the reinsertion of lithium ($Li_{1.6}$(r)) maxima associated with hydroxyl groups decrease strongly,

Table 3. Structural Parameters Obtained from EXAFS Spectra of the First Shell of Oxygen Atoms and the Second Shell of Manganese Atoms with Fixed Coordination Numbers, $N_1 = 6.0$ and $N_2 = 4.8$, for Parent, Delithiated, and Relithiated $Li_{1.6}Mn_{1.6}O_4$[a]

	Mn−O		Mn−Mn	
	R_1 (Å)	σ_1 (Å)	R_2 (Å)	σ_2 (Å)
$Li_{1.6}$(p)	1.91(8)	0.065	2.86(6)	0.067
$Li_{1.6}$(d)	1.91(7)	0.066	2.85(8)	0.077
$Li_{1.6}$(r)	1.92(1)	0.068	2.87(3)	0.072
$Li_{1.33}$(p)[b]	1.90(8)		2.87(3)	
$Li_{1.33}$(d)[b]	1.90(2)		2.85(8)	
$Li_{1.33}$(r)[b]	1.91(1)		2.87(5)	

[a] Figures in brackets are not significant within accuracy of EXAFS interatomic distances (∼0.01 Å). [b] Taken from ref 13.

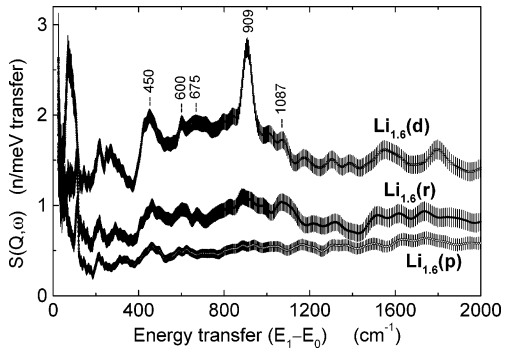

Figure 5. Inelastic neutron scattering spectra of $Li_{1.6}Mn_{1.6}O_4$ ($Li_{1.6}$(p)), acid-washed ($Li_{1.6}$(d)), and lithium-reinserted ($Li_{1.6}$(r)) samples. Statistical errors are plotted as vertical lines.

(16) Howard, J.; Tomkinson, J.; Eckert, J.; Goldstone, J.; Taylor, A. D. *J. Chem. Phys.* **1983**, *78*, 3150.
(17) Fillaux, F.; Cachet, C. H.; Ouboumour, H.; Tomkinson, J.; Levy-Clement, C.; Yu, L. T. *J. Electrochem. Soc.* **1993**, *140*, 585.
(18) Ammundsen, B.; Burns, G. R.; Islam, M. S.; Kanoh, H.; Rozière, J. *J. Phys. Chem. B* **1999**, *103*, 5175.

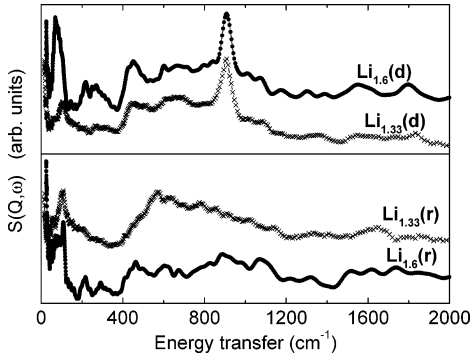

Figure 6. IINS spectra of delithiated and relithiated materials obtained from $Li_{1.6}Mn_{1.6}O_4$ ($Li_{1.6}$(d) and $Li_{1.6}$(r), respectively) compared to those materials obtained from $Li_{1.33}Mn_{1.67}O_4$ ($Li_{1.33}$(d) and $Li_{1.33}$(r)).

but they are still visible. The background is weaker than in the lithium-extracted sample but higher than that of the parent sample, and the peaks associated with water libration and vibrations of the water-activated MnO_6 are also more pronounced than in the parent. Some protons are therefore retained after the reinsertion of lithium, mainly as structural water but also as hydroxyl species. On relithiation, the decrease of the peak at 909 cm^{-1} is higher than that at 1087 cm^{-1} (compare $Li_{1.6}$(r) and $Li_{1.6}$(d) spectra). If it is assumed that each maximum corresponds to a different lattice site, this suggests that the extraction of the smaller amount of protons occupying the second site is less favorable. Muon spin relaxation (μSR) has shown two possible muon (μ^+) sites in the related Li-rich phase $Li_{1.33}Mn_{1.67}O_4$.[19] Since μ^+ behaves as a light proton, this suggests that protons may also occupy two different lattice sites in the $Li_{1.6}Mn_{1.6}O_4$, and μSR experiments are planned on this new phase.

On the other hand, the overall position of the rising XANES edge remains essentially unchanged throughout the lithium extraction and reinsertion processes (see Figure 1), being the manganese atoms mainly Mn^{IV} in the parent, delithiated, and relithiated $Li_{1.6}Mn_{1.6}O_4$. Both the presence of hydroxyl groups (IINS results) in the lithium-extracted sample and the lack of Mn^{III} atoms (XANES results) allow us to reject any electron-transfer reaction and conclude that lithium insertion/extraction is mainly a lithium-by-proton-exchange mechanism in this new lithium-rich spinel manganate.

Comparison with the Phase $Li_{1.33}Mn_{1.67}O_4$ and Possible Location of the Extra Lithium in $Li_{1.6}Mn_{1.6}O_4$. $Li_{1.33}Mn_{1.67}O_4$ has been previously considered the end-member of the spinel-structured lithium-rich series $Li_{1+x}Mn_{2-x}O_4$. This phase was comprehensively studied by X-ray absorption spectroscopy and neutron diffraction, and the cubic spinel structure with Li in 8a and 16d Mn vacant sites ($Fd\bar{3}m$ space group) is well-established.[3,7,13] The role of protons in lithium extraction and reinsertion was also studied by IINS in $Li_{1.33}$(p), $Li_{1.33}$(d), and $Li_{1.33}$(r) materials corresponding to $Li_{1.33}Mn_{1.67}O_4$.[6]

Figure 6 compares the IINS spectra of the lithium-extracted $Li_{1.6}Mn_{1.6}O_4$ and $Li_{1.33}Mn_{1.67}O_4$ (top) and both relithiated (bottom) materials. Both delithiated spectra show the same pattern of intensity in the energy region of interest (from 400 to 1200 cm^{-1}) with the very intense maximum at 909 cm^{-1} dominating the spectra (γ(OH)). It is noted that the peak corresponding to vibrations of the activated MnO_6 octahedra (450 cm^{-1}) is more pronounced in $Li_{1.6}$(d) than in $Li_{1.33}$(d). Differences are more significant between the spectra of relithiated samples: for $Li_{1.33}$(r) the main feature of the IINS spectrum is a broad contribution between 400 and 1200 cm^{-1}, while the peak corresponding both to hydroxyl and to MnO_6 vibrations disappear below this background. For $Li_{1.6}$(r) vibrations of activated MnO_6 octahedra are clearly observed and the signals from γ(OH) are weak but still visible. Although the same types of protonic species are formed in both delithiated materials, this result shows there to be some differences in the proton uptake between these two lithium-rich spinel manganese oxides. Differences can be also observed in the peaks below 300 cm^{-1}, which corresponds to lattice vibration modes.[7] The higher amount of Li in $Li_{1.6}Mn_{1.6}O_4$ may influence the stability of some protonic species with respect to others, and for that reason the lithium exchange capacity and lithium uptake from Li-enriched seawater is higher for this new spinel manganese oxide. The existence of inserted protons which cannot be reexchanged for lithium has been proposed to explain that reverse lithium-proton exchange proceeds only to ~60% from $Li_{1.33}Mn_{1.67}O_4$.[6]

On the other hand, the above results from X-ray absorption spectroscopy show a very similar behavior of the local structure of both lithium-rich phases when the lithium is extracted and reinserted. In both parent samples ($Li_{1.33}Mn_{1.67}O_4$ and $Li_{1.6}Mn_{1.6}O_4$), the average oxidation state of manganese is 4+, and it remains unaffected when Li is extracted and reinserted. The same type of features occurs on the Mn K-edge (XANES), and they show the same evolution when the lithium is extracted and reinserted. All this indicates an ion exchange mechanism for the extraction/insertion of lithium in both phases. The EXAFS oscillations are also very similar, not only those corresponding to the first oxygen and second manganese shells of atoms but also the medium-range order, as can be observed in Figure 7. Therefore, EXAFS and XANES are both strongly in favor of a cubic spinel local structure for $Li_{1.6}Mn_{1.6}O_4$. The existence of a layered structure (hexagonal lattice with cation deficiency)[5] can be excluded on the basis of these results.

Nevertheless, the ratio of cations to anions derived from $Li_{1.6}Mn_{1.6}O_4$ chemical composition in this new spinel lithium-rich phase is not typical for a spinel phase (3:4). Either the existence of interstitial cations or oxygen vacancies in the cubic spinel structure must be then considered. As described above, $Li_{1.6}Mn_{1.6}O_4$ and $Li_{1.33}Mn_{1.67}O_4$ have very similar XANES and EXAFS spectra, as well as identical trends in structural evolution on lithium extraction and reinsertion. However, both lithium-by-protons and protons-by-lithium exchanges are more effective in the new lithium-rich spinel. Lithium and hydrogen atoms cannot be directly detected by X-ray absorption experiments, and thus the extra lithium has not been located, but neutron diffraction experiments could be expected to provide further information.

(19) Ariza, M. J.; Jones, D. J.; Rozière, J.; Lord, J. S.; Ravot, D. *J. Phys. Chem. B* **2003**, *107*, 6003.

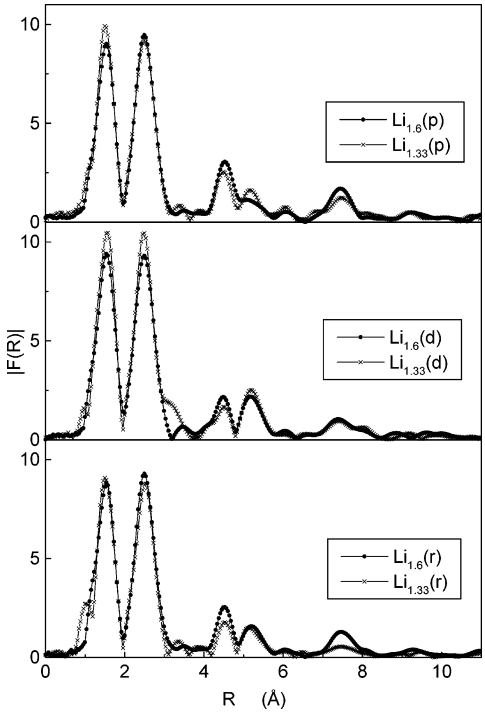

Figure 7. Comparison of the radial distribution function of the parent (top), delithiated (middle), and relithiated (bottom) materials extracted from $Li_{1.6}Mn_{1.6}O_4$ and $Li_{1.33}Mn_{1.67}O_4$.

Conclusions

Lithium extraction/insertion in the new lithium-rich manganese oxide $Li_{1.6}Mn_{1.6}O_4$ occurs via lithium−proton exchange. Inelastic neutron scattering spectroscopy has shown −OH groups and structural water in the sample delithiated by acid washing. This water may be located in lamellar-like regions of the defect structure.[7] Some water and −OH groups remain in the structure when the lithium is reinserted. The exchange mechanism is similar to that of $Li_{1.33}Mn_{1.67}O_4$, the previously considered end-member of the series of spinel lithium-rich manganese oxides, but IINS has confirmed that the extraction of protons and reinsertion of Li^+ is more effective in $Li_{1.6}Mn_{1.6}O_4$, in agreement with the improved lithium uptake properties shown by the lithium-extracted form.

X-ray absorption spectroscopy of $Li_{1.6}Mn_{1.6}O_4$ samples has shown no overall shift of the Mn absorption edge after lithium extraction/reinsertion. The edge position indicates that the oxidation state of manganese is predominantly 4+ in the parent, delithiated, and relithiated samples, which confirms the ion exchange mechanism for lithium extraction and reinsertion.

$Li_{1.6}Mn_{1.6}O_4$ adopts a spinel structure, despite its atypical cation/anion ratio. In particular, the two features in the rising edge of XANES spectra are highly typical of the spinel structure, and structural parameters obtained by EXAFS also are highly compatible with the spinel structure. The trend of structural evolution on lithium exchange is identical to that of $Li_{1.33}Mn_{1.67}O_4$, but extra lithium in the parent material influence the effectiveness of lithium extraction and reinsertion. All these results are more compatible with the existence of interstitial cations than with an oxygen-deficient spinel structure, although such light cations (lithium and protons) cannot be located by X-ray absorption.

Acknowledgment. We thank Dr. Daniel Colognesi for his very useful help on the IINS data extraction process. M.J.A. thanks the Spanish government (MAT2004-03581 project and Ramon y Cajal program) for financial support.

CM052214R